

Supporting Information

Density–nematic coupling in isotropic linear polymers: acoustic and osmotic birefringence

Aleksandar Popadić,¹ Daniel Svenešek,^{2,*} Rudolf Podgornik,^{2,3,4,5} and Matej Praprotnik¹

¹Laboratory for Molecular Modeling, National Institute of Chemistry, SI-1001 Ljubljana, Slovenia

²Department of Physics, Faculty of Mathematics and Physics, University of Ljubljana, SI-1000 Ljubljana, Slovenia

³Department of Theoretical Physics, J. Stefan Institute, SI-1000 Ljubljana, Slovenia

⁴School of Physical Sciences and Kavli Institute for Theoretical Sciences, University of Chinese Academy of Sciences, Beijing 100049, China

⁵CAS Key Laboratory of Soft Matter Physics, Institute of Physics, Chinese Academy of Sciences, Beijing 100190, China

I. TENSORIAL CONSERVATION LAW

A linear polymer is modeled as a continuous WLC presented by the microscopic density field of the polymer length

$$\rho^{\text{mic}}(\mathbf{x}) = \sum_{\alpha} \int_{\mathbf{x}^{\alpha}(s)} ds \delta(\mathbf{x} - \mathbf{x}^{\alpha}(s)), \quad (1)$$

i.e., the total length of the polymer per unit volume, where $\mathbf{x}^{\alpha}(s)$ is the contour of the chain α in natural parametrization. For brevity we will be omitting the superscript α and the sum \sum_{α} over the chains. The continuity of $\mathbf{x}(s)$ stands for the unbroken connectivity of the polymer chains. A microscopic traceless polymer nematic tensor field can be defined as

$$J_{ij}^{\text{mic}}(\mathbf{x}) = \int_{\mathbf{x}(s)} ds \delta(\mathbf{x} - \mathbf{x}(s)) \frac{3}{2} [t_i(s)t_j(s) - \frac{1}{3}\delta_{ij}] \equiv \tilde{J}_{ij}^{\text{mic}}(\mathbf{x}) - \frac{1}{2}\delta_{ij}\rho^{\text{mic}}(\mathbf{x}), \quad (2)$$

where $\mathbf{t}(s) = d\mathbf{x}(s)/ds$ is the unit tangent on the chain.

Taking a divergence of Equation (2),

$$\partial_j (J_{ij}^{\text{mic}} + \frac{1}{2}\delta_{ij}\rho^{\text{mic}}) = \frac{3}{2} \int_{\mathbf{x}(s)} ds \frac{dx_i(s)}{ds} \frac{dx_j(s)}{ds} \frac{\partial}{\partial x_j} \delta(\mathbf{x} - \mathbf{x}(s)), \quad (3)$$

using $\frac{dx_j(s)}{ds} \frac{\partial}{\partial x_j} \delta(\mathbf{x} - \mathbf{x}(s)) = -\frac{dx_j(s)}{ds} \frac{\partial}{\partial x_j(s)} \delta(\mathbf{x} - \mathbf{x}(s)) = -\frac{d}{ds} \delta(\mathbf{x} - \mathbf{x}(s))$ and integrating by parts, we get

$$\partial_j (J_{ij}^{\text{mic}} + \frac{1}{2}\delta_{ij}\rho^{\text{mic}}) = \frac{3}{2} [t_i(0)\delta(\mathbf{x} - \mathbf{x}(0)) - t_i(L)\delta(\mathbf{x} - \mathbf{x}(L))] + \frac{3}{2} \int_{\mathbf{x}(s)} ds \frac{d^2 x_i(s)}{ds^2} \delta(\mathbf{x} - \mathbf{x}(s)), \quad (4)$$

where $s = 0$ and $s = L$ corresponds to the beginning and ending of a chain, respectively. In the absence of polar order, this identification is arbitrary and the beginning and ending tangents can be unified into a single type of tangents \mathbf{t}^n always pointing inwards, such that $t_i(0)\delta(\mathbf{x} - \mathbf{x}(0)) - t_i(L)\delta(\mathbf{x} - \mathbf{x}(L)) = t_i^n(0)\delta(\mathbf{x} - \mathbf{x}(0)) + t_i^n(L)\delta(\mathbf{x} - \mathbf{x}(L))$.

Writing a microscopic field $\mathbf{F}^{\text{mic}}(\mathbf{x})$, i.e., Equations (1) to (2) and also the last term of Equation (4), in the form

$$\mathbf{F}^{\text{mic}}(\mathbf{x}) = \int_{\mathbf{x}(s)} ds \delta(\mathbf{x} - \mathbf{x}(s)) \mathbf{f}(\mathbf{x}(s)), \quad (5)$$

coarse-graining it to the mesoscopic volume V centered at \mathbf{x} (denoted by $\overline{}$) gives the corresponding mesoscopic field [1]

$$\mathbf{F}(\mathbf{x}) = \overline{\mathbf{F}^{\text{mic}}}(\mathbf{x}) = \frac{1}{V} \int_{V(\mathbf{x})} d^3x' \mathbf{F}^{\text{mic}}(\mathbf{x}') = \frac{1}{V} \int_{\mathbf{x}(s) \in V(\mathbf{x})} ds \mathbf{f}(\mathbf{x}(s)) = \frac{L(\mathbf{x})}{V} \frac{1}{L(\mathbf{x})} \int_{\mathbf{x}(s) \in V(\mathbf{x})} ds \mathbf{f}(\mathbf{x}(s)), \quad (6)$$

* daniel.svensek@fmf.uni-lj.si

where $L(\mathbf{x}) = \int_{\mathbf{x}(s) \in V(\mathbf{x})} ds \equiv N(\mathbf{x})l_0$ is the total length of the chain within the volume V , which can be expressed in terms of an arbitrary segment length l_0 and the number N of these segments within the volume. Hence, the mesoscopic field can be written as

$$\mathbf{F}(\mathbf{x}) = \rho(\mathbf{x})l_0 \bar{\mathbf{f}}(\mathbf{x}), \quad (7)$$

where $\rho(\mathbf{x}) = N(\mathbf{x})/V$ is the mesoscopic volume number density of the segments and

$$\bar{\mathbf{f}}(\mathbf{x}) = \frac{1}{L(\mathbf{x})} \int_{\mathbf{x}(s) \in V(\mathbf{x})} ds \mathbf{f}(\mathbf{x}(s)) \quad (8)$$

is the mesoscopic average of $\mathbf{f}(\mathbf{x}(s))$.

Applying this coarse-graining procedure to Equation (4), where in particular $\overline{\rho^{\text{mic}}} = \rho l_0$, $\overline{J_{ij}^{\text{mic}}} \equiv J_{ij} = \rho l_0 Q_{ij}$, and bearing in mind that the coarse-graining and ∇ commute, we get an equation for continuum mesoscopic fields — the tensorial conservation law

$$\partial_j [\rho(Q_{ij} + \frac{1}{2}\delta_{ij})] = \frac{3}{2}\frac{1}{l_0}g_i + \frac{3}{2}\rho k_i, \quad (9)$$

where \mathbf{Q} is the nematic order tensor,

$$Q_{ij}(\mathbf{x}) = \frac{1}{L(\mathbf{x})} \int_{\mathbf{x}(s) \in V(\mathbf{x})} ds \frac{3}{2} [t_i(s)t_j(s) - \frac{1}{3}\delta_{ij}], \quad (10)$$

$\mathbf{g}(\mathbf{x}) = \overline{\mathbf{t}^n(0)\delta(\mathbf{x} - \mathbf{x}(0)) + \mathbf{t}^n(L)\delta(\mathbf{x} - \mathbf{x}(L))}$ is the mesoscopic density of chain-end tangents and

$$\mathbf{k}(\mathbf{x}) = \frac{1}{L(\mathbf{x})} \int_{\mathbf{x}(s) \in V(\mathbf{x})} ds \frac{d^2\mathbf{x}(s)}{ds^2} \quad (11)$$

is the mesoscopic average chain curvature vector.

II. CORRELATION FUNCTIONS OF COLLECTIVE FLUCTUATIONS

We present the results for fluctuations of the isotropic linear polymer system in the continuum description. A minimal free-energy density of the isotropic phase taking into account density variations, nematic fluctuations satisfying $\delta Q_{kk} = 0$ by definition, and the constraint is

$$f = \frac{1}{2}B \left(\frac{\delta\rho}{\rho_0}\right)^2 + \frac{1}{2}B' \left(\frac{\partial_i\delta\rho}{\rho_0}\right)^2 + \frac{1}{2}A(\delta Q_{ij})^2 + \frac{1}{2}L(\partial_k\delta Q_{ij})^2 + \frac{1}{2}G\left(\frac{2}{3}\rho_0 l_0\right)^2 \left[\partial_j\delta Q_{ij} + \frac{1}{2}\partial_i\left(\frac{\delta\rho}{\rho_0}\right)\right]^2, \quad (12)$$

where B is the bulk modulus, ρ_0 is the volume number density of monomers, A is the “nematic order stiffness” and B' and L (the nematic elastic constant) are penalizing ρ and \mathbf{Q} gradients. The density and nematic correlation lengths are $\xi_\rho \sim \sqrt{B'/B}$ and $\xi \sim \sqrt{L/A}$, respectively. The constraint due to the tensorial conservation law is taken into account by a quadratic potential penalizing its sources, where $G\left(\frac{2}{3}\rho_0 l_0\right)^2 \equiv \tilde{G}$ is the strength of the constraint. A minimal model for G with the final result is developed in Section IV.

In Fourier space, $u(\mathbf{q}) = \int d^3r u(\mathbf{r})e^{-i\mathbf{q}\cdot\mathbf{r}}$, and with $\delta\rho/\rho_0 \equiv \delta\tilde{\rho}$, the free-energy density (Equation (12)) is

$$f(\mathbf{q}) = \frac{1}{2}\tilde{B}|\delta\tilde{\rho}|^2 + \frac{1}{2}(A + Lq^2)|\delta Q_{ij}|^2 + \frac{1}{2}\tilde{G}|q_j\delta Q_{ij} + \frac{1}{2}q_i\delta\tilde{\rho}|^2, \quad (13)$$

where $\tilde{B} = B + B'q^2$. The free energy is $F = \int d^3r f = (1/V)\sum_{\mathbf{q}} f(\mathbf{q})$, where V is the volume of the system. By equipartition, the energy corresponding to an individual quadratic contribution $f_i(\mathbf{q})$ to Equation (13) is $\langle f_i(\mathbf{q}) \rangle / V = k_B T / 2$, with k_B the Boltzmann constant and T the temperature.

To determine the fluctuation amplitudes, the quadratic form in Equation (13) is diagonalized. Since the system is isotropic, without loss of generality we may assume $\mathbf{q} = q\hat{\mathbf{e}}_z$, where z is an arbitrarily chosen direction defining the z axis of the coordinate system. Axes x and y are then fixed arbitrarily and all results at a given q must be invariant to rotations of the tensors in the xy plane. Since \mathbf{Q} is traceless by definition, only two of δQ_{xx} , δQ_{yy} , and δQ_{zz} are independent. Conforming to the symmetry of the problem, we put $\delta Q_{zz} = -(\delta Q_{xx} + \delta Q_{yy})$ and take δQ_{xx} ,

δQ_{yy} as the variables. Moreover, for the remaining three variables we take δQ_{xy} , δQ_{xz} , δQ_{yz} , which represent also their transposes and will thus give twofold free-energy contributions. With that, the diagonalized free-energy form of Equation (13) is

$$\begin{aligned} f(q) &= \frac{1}{2}(A + Lq^2) \left(2|\delta Q_{xy}|^2 + |\delta Q_{xx} - \delta Q_{yy}|^2 \right) \\ &+ \left[A + \left(L + \frac{1}{2}\tilde{G} \right) q^2 \right] \left(|\delta Q_{xz}|^2 + |\delta Q_{yz}|^2 \right) \\ &+ \frac{\lambda^+}{v_+^2} |a_+ \delta \tilde{\rho} + \delta Q_{zz}|^2 + \frac{\lambda^-}{v_-^2} |a_- \delta \tilde{\rho} + \delta Q_{zz}|^2, \end{aligned} \quad (14)$$

where we reverted to δQ_{zz} in the last two terms. The expressions $v_{\pm}^2 = 2 + a_{\pm}^2$,

$$a_{\pm} = \frac{1}{4\tilde{G}q^2} \left\{ 4\tilde{B} - 12A - q^2(7\tilde{G} + 12L) \pm \sqrt{\left[4\tilde{B} - 12A - q^2(7\tilde{G} + 12L) \right]^2 + 32\tilde{G}q^4} \right\}, \quad (15)$$

$$\lambda^{\pm} = \frac{1}{16} \left\{ 4\tilde{B} + 12A + 3q^2(3\tilde{G} + 4L) \pm \sqrt{\left[4\tilde{B} - 12A - q^2(7\tilde{G} + 12L) \right]^2 + 32\tilde{G}q^4} \right\} \quad (16)$$

are real and the stability condition requires $\lambda^{\pm} > 0$.

The autocorrelations of the variables that appear quadratically in Equation (14) follow immediately from equipartition, Equations (20) and (21). The fluctuation $\delta Q_{xx} - \delta Q_{yy}$ leaves δQ_{zz} unaltered and its free-energy cost is the same as that of δQ_{xy} (note the twofold contribution of this latter off-diagonal term) — as it must be to recover the isotropy in the xy plane. As such, it does not bring anything new.

The last two terms in Equation (14) represent the contributions of two coupled fluctuation modes, i.e., it is just the component δQ_{zz} (and thus also the sum $\delta Q_{xx} + \delta Q_{yy}$) that is coupled to density. Alternatively, one can write those terms as

$$\frac{\lambda^+ \lambda^- (a_+ - a_-)^2}{\lambda^+ v_-^2 + \lambda^- v_+^2} |\delta \tilde{\rho}|^2 + |\dots \delta Q_{zz} + \dots \delta \tilde{\rho}|^2 \quad (17)$$

or

$$\frac{\lambda^+ \lambda^- (a_+ - a_-)^2}{\lambda^+ v_-^2 a_+^2 + \lambda^- v_+^2 a_-^2} |\delta Q_{zz}|^2 + |\dots \delta \tilde{\rho} \dots \delta Q_{zz}|^2 \quad (18)$$

and therefrom calculate $\langle |\delta Q_{zz}|^2 \rangle$ and $\langle |\delta \tilde{\rho}|^2 \rangle$.

Finally, using $\langle |\delta Q_{zz}|^2 \rangle$ and $\langle |\delta \tilde{\rho}|^2 \rangle$ together with the average of one of the last terms of Equation (14), e.g.,

$$\left\langle |a_{\pm} \delta \tilde{\rho} + \delta Q_{zz}|^2 \right\rangle = \frac{k_B T}{2} V \frac{v_{\pm}^2}{\lambda^{\pm}} \quad (19)$$

which we are not giving explicitly, one arrives at the cross-correlation.

Whence, the complete set of Fourier-component thermodynamic correlation functions in space is

$$\frac{1}{N_0} \langle |\delta Q_{xy}|^2 \rangle = \frac{k_B T}{2} \frac{1}{\rho_0} \frac{1}{A + Lq^2} \quad (20)$$

$$\frac{1}{N_0} \langle |\delta Q_{\{xz,yz\}}|^2 \rangle = \frac{k_B T}{2} \frac{1}{\rho_0} \frac{1}{A + \left(L + \frac{1}{2}\tilde{G} \right) q^2} \quad (21)$$

$$\frac{1}{N_0} \langle |\delta Q_{zz}|^2 \rangle = \frac{k_B T}{2} \frac{4}{\rho_0} \left[3A + \left(3L + \frac{8\tilde{G}\tilde{B}}{4\tilde{B} + \tilde{G}q^2} \right) q^2 \right]^{-1} \quad (22)$$

$$\frac{1}{N_0} \langle |\delta \tilde{\rho}|^2 \rangle = \frac{k_B T}{2} \frac{8}{\rho_0} \left[4\tilde{B} + \frac{3\tilde{G}(A + Lq^2)q^2}{3A + (3L + 2\tilde{G})q^2} \right]^{-1} \quad (23)$$

$$\frac{1}{2N_0} \langle \delta \tilde{\rho}^* \delta Q_{zz} + \delta \tilde{\rho} \delta Q_{zz}^* \rangle = -\frac{k_B T}{2} \frac{1}{\rho_0} \frac{8\tilde{G}q^2}{12A\tilde{B} + [12\tilde{B}L + (3A + 8\tilde{B})\tilde{G}]q^2 + 3\tilde{G}Lq^4}. \quad (24)$$

III. MESOSCOPIC WLC MODEL AND NUMERICAL SIMULATION DETAILS

In the MC simulations, we use a recently developed mesoscopic model of discrete WLCs [2, 3]. The modeled system contains N_c WLCs comprised of N_s linearly connected segments of fixed length l_0 . Consecutive segments are subjected to a standard angular potential

$$U_b = -\epsilon \mathbf{u}^{i,s} \cdot \mathbf{u}^{i,s+1}, \quad (25)$$

where $\mathbf{u}^{i,s}$ is the unit vector along the s -th segment of the i -th chain and ϵ controls the WLC bending stiffness. Non-bonded interactions between segments are introduced via the potential $U_{nb} = \kappa U(r_{ij}^{st})$, where κ is the strength of the isotropic repulsion between the segments and $U(r_{ij}^{st}) = C_0 \Theta(2\sigma - r_{ij}^{st}) [4\sigma + r_{ij}^{st}] [2\sigma - r_{ij}^{st}]^2$ represents the overlap of two spherical clouds centered on the s -th and t -th segments of the i -th and j -th chain, respectively; r_{ij}^{st} is the distance between the segments and σ controls the interaction range as indicated by the Heaviside function Θ . To verify the predictions of the macroscopic theory it is sufficient to employ a generic model with a single ‘‘microscopic’’ length scale. Hence, we set $\sigma = l_0$, although other choices are possible [4, 5] when modeling actual materials. The normalization constant of $U(r_{ij}^{st})$ is set to $C_0 = 3l_0^3/(64\pi\sigma^6)$. We empirically set $\kappa = 7.58 k_B T$ [2]. Several molecular flexibilities ranging from $\epsilon = 0$ to $\epsilon = 13.136 k_B T$ are addressed, corresponding to decreasing flexibility of the chains. The MC algorithm utilizes a combination of standard random monomer displacement and slithering snake moves [6]. In addition, every $N_0 = N_c N_s$ random displacement and slithering snake moves, a volume fluctuation move at pressure $P l_0^3/(k_B T) = 2.87$ is employed [7].

The fluctuations of any variables $\delta a(\mathbf{q}) = \sum_s a_s e^{-i\mathbf{q}\cdot\mathbf{r}^s}$ and $\delta b(\mathbf{q}) = \sum_s b_s e^{-i\mathbf{q}\cdot\mathbf{r}^s}$ are extracted via their correlation functions,

$$\frac{1}{2N_0} [\langle \delta a(\mathbf{q}) \delta b(-\mathbf{q}) \rangle + \langle \delta a(-\mathbf{q}) \delta b(\mathbf{q}) \rangle] = \frac{1}{N_0} \left\langle \left[\sum_s a_s \cos(\mathbf{q} \cdot \mathbf{r}^s) \right] \left[\sum_s b_s \cos(\mathbf{q} \cdot \mathbf{r}^s) \right] + \left[\sum_s a_s \sin(\mathbf{q} \cdot \mathbf{r}^s) \right] \left[\sum_s b_s \sin(\mathbf{q} \cdot \mathbf{r}^s) \right] \right\rangle, \quad (26)$$

where $s = 1 \dots N_0$ runs over the segments of all chains and \mathbf{r}^s are their positions. For segment density fluctuations $\delta\rho$ we have $a_s = 1$, and for the nematic fluctuations δJ_{ij} we have $a_s = (3u_i^s u_j^s - \delta_{ij})/2$. Note that the coarse graining does not affect the $\mathbf{q} \rightarrow 0$ Fourier components, or in other words, the $\mathbf{q} \rightarrow 0$ components of the extracted discrete variables are automatically coarse-grained. Hence, the long-wavelength correlations (Equation (26)) computed from the simulation data can be directly compared to the predictions of the continuum theory.

The ensemble volume is free to fluctuate and the set of \mathbf{q} vectors is determined by the current box size. Since the system is isotropic, all quantities depend only on the magnitude $|\mathbf{q}| = q$. We average them over spherical shells with thickness $\Delta q \sim 2\pi/\langle L \rangle$, taking care that also the smallest shells ($q \rightarrow 0$) are adequately populated. In an isotropic system, the isotropic symmetry of non-scalar quantities is broken only by the direction \mathbf{q} , which is exploited in the averaging procedure as follows. For every \mathbf{q} , we set the coordinate system such that $\mathbf{q} = q\hat{\mathbf{e}}_z$, while

$$\hat{\mathbf{e}}_x = \frac{\hat{\mathbf{e}}_{x'} - (\hat{\mathbf{e}}_{x'} \cdot \hat{\mathbf{e}}_z)\hat{\mathbf{e}}_z}{|\hat{\mathbf{e}}_{x'} - (\hat{\mathbf{e}}_{x'} \cdot \hat{\mathbf{e}}_z)\hat{\mathbf{e}}_z|}$$

and $\hat{\mathbf{e}}_y = \hat{\mathbf{e}}_z \times \hat{\mathbf{e}}_x$, where $\hat{\mathbf{e}}_{x'}$ is aligned with the simulation box. With that, for the component δJ_{zz} we have $a_s = [3(\mathbf{u}^s \cdot \hat{\mathbf{e}}_z)^2 - 1]/2$ and for the components $\delta J_{\{x,y\}z}$ we have $a_s = 3(\mathbf{u}^s \cdot \hat{\mathbf{e}}_{\{x,y\}})(\mathbf{u}^s \cdot \hat{\mathbf{e}}_z)/2$.

The computed correlations are then averaged over collected configurations. When calculating averages, we use block-averaging with block size τ , where τ is the number of MC steps needed to decorrelate the end-to-end vector of the WLC [8].

IV. THEORETICAL MODEL OF THE SOURCES

In this additional step, we build a theoretical model to predict the coupling strength G on the basis of length and flexibility of the chains. Similar to what has been done in Ref. [3], we resort to a minimal model of the sources of the tensorial continuity equation in the sense that i) we treat both macroscopic sources as composed of independent microscopic contributions to chain-end tangent density \mathbf{g} (Section IV A) and average chain curvature \mathbf{k} (Section IV B), respectively, and ii) we combine both sources into a single unified source $\mathbf{h} = \mathbf{g} + \rho_0 l_0 \mathbf{k}$ with a properly weighted relative composition (Section IV C). Only this latter case allows the tensorial constraint to be taken into account simply by a

penalty potential term in the free-energy density (Equation (12)), which means that no additional variables for the sources are required.

Thus, we shall construct the nonequilibrium free energy cost of the sources in the simplest possible way and in lowest, quadratic order of the sources. Since $\mathbf{g} = 0$ in equilibrium, the variation $\delta\mathbf{g}$ of the density of end tangents involves only the variation of their average orientation, and does not involve the variation of their density. (This is true also in the nematic phase.) Similarly, the equilibrium average chain curvature \mathbf{k} is zero, so the variation of $\rho\mathbf{k}$ does not involve the variation of the density. (This is true also in the nematic phase, provided it is not bent.)

A. End tangents

We construct a purely entropic nonequilibrium orientational free energy of orientationally independent end tangents, taking into account their dipolar ordering that results in nonzero \mathbf{g} . The orientational part of the entropic free energy is then

$$F(p_1) = -TS(p_1) = k_B T \int d\Omega p(\Omega) \ln p(\Omega), \quad (27)$$

where $p(\Omega) = p_0 + p_1 \sqrt{3/2} P_1(\cos\theta)$ is the orientational distribution function of end tangents with respect to the solid angle Ω , $P_1(\cos\theta) = \cos\theta$ is the first Legendre polynomial and $p_0 = 1/2$ is fixed by the normalization $\int_{-1}^1 d(\cos\theta) p(\Omega) = 1$. In the isotropic system, the orientation of the z axis of the spherical coordinate system is arbitrary. Moreover, $p_1 = \sqrt{3/2} \langle \cos\theta \rangle$ is the dipole moment of end tangent orientations (a nonzero p_1 means a nonzero \mathbf{g}), which is the only parameter of the orientational distribution.

One can verify that the first derivative $\left. \frac{dF}{dp_1} \right|_{p_1=0} = 0$, so that the free energy is indeed minimum for the isotropic orientational distribution of end tangents. Hence, for a single chain end, we have

$$\Delta F(p_1) = \frac{1}{2} \left. \frac{d^2 F}{dp_1^2} \right|_{p_1=0} p_1^2 = \frac{1}{2} 2k_B T p_1^2. \quad (28)$$

For many independent chain ends with density ρ_0^\pm , the free-energy density is thus

$$\Delta f = \frac{1}{2} 2\rho_0^\pm k_B T p_1^2 = \frac{1}{2} \frac{3k_B T}{\rho_0^\pm} g^2. \quad (29)$$

where we took into account that with respect to a given direction $g = \rho_0^\pm \langle \cos\theta \rangle = \rho_0^\pm \sqrt{2/3} p_1$. This is thus the entropic free energy cost of the density $g = |\mathbf{g}|$ of independent tangents of chain ends with number density ρ_0^\pm . Not unexpectedly, it has the same $1/\rho_0^\pm$ dependence as the entropic free-energy density of the source of the vectorial constraint [3].

B. Chain curvature

We shall construct a nonequilibrium free-energy density of nonzero local average curvature of the chains. The bending free energy of a single WLC with nearest-neighbour bending interactions (which also corresponds to the angular potential used in the microscopic simulation) is $\Delta F = \sum_i \Delta F_i$, with

$$\Delta F_i = \frac{1}{2} \epsilon l_0^2 |\mathbf{k}^i|^2 = \epsilon (1 - \cos\theta_{i,i+1}), \quad (30)$$

where $\mathbf{k}^i = (\mathbf{u}^{i+1} - \mathbf{u}^i)/l_0$, \mathbf{u}^i is the unit vector along the i -th segment of the chain, and $\cos\theta_{i,i+1} = \mathbf{u}^i \cdot \mathbf{u}^{i+1}$. Thus, considering only the bending free energy of Equation (30), the individual microscopic curvature elements, corresponding to individual monomer joints, are independent. The relevance of this independent joint assumption in the actual system including also non-bonded interactions is demonstrated in Section V. If the chain segments are bent only slightly, i.e., when $k_B T \ll \epsilon$, then the two components of \mathbf{k}^i can be as usual considered ranging from $-\infty$ to ∞ , such that equipartition holds and

$$\langle (k_1^i)^2 \rangle = \frac{k_B T}{\epsilon l_0^2}, \quad (31)$$

where k_1^i is one of the components. In the continuum limit, $\mathbf{k}(s) = d\mathbf{t}/ds$ is the local chain curvature vector and the free energy is $\Delta F = \frac{1}{2}K \int ds k(s)^2$, where s is the arclength along the chain and $K = \epsilon l_0$ is the bending rigidity of the continuous WLC, if one disregards the rather small influence of the non-bonded interactions on the flexibility of the discrete WLC.

To arrive at the free energy of the collective (average) chain curvature \mathbf{k} , one has to find the configuration of \mathbf{k}^i 's that corresponds to the most complete equilibrium [9, pp. 335, 398] at a given \mathbf{k} , e.g., for segment pairs that are on average perpendicular to \mathbf{k} this would simply mean $\mathbf{k}^i = \mathbf{k}$. In the isotropic system, however, the segments point in all directions. Let $\mathbf{k} = k\hat{\mathbf{e}}_z$. By symmetry, the segment pairs oriented along z , i.e., $\theta = 0$, are not bend on average and therefore do not contribute either to \mathbf{k} or to the free energy. The contributions of the segment pairs lying in the xy plane ($\theta = \pi/2$) are on the other hand maximum (and equal). We shall assume that the magnitude of the joint's curvature vector $\mathbf{k}_0 = -k_0\hat{\mathbf{e}}_\theta$ goes as $k_0 \propto \sin\theta$, such that its contribution to the macroscopic curvature is $\mathbf{k}_0 \cdot \hat{\mathbf{e}}_z \propto \sin^2\theta$. Requiring that its solid angle average is k , we get $k_0(\theta) = \frac{3}{2}k \sin\theta$. For a constant density of monomers ρ_0 , the corresponding effective curvature free-energy density is then obtained by averaging Equation (30) over the solid angle, with the result

$$\Delta f(k) = \frac{1}{2} \frac{3}{2} \epsilon l_0^2 \rho_0 k^2 = \frac{1}{2} \frac{3\epsilon l_0^2}{2\rho_0} (\rho_0 k)^2, \quad (32)$$

where k is the macroscopic (average) chain curvature in an arbitrary direction of the isotropic system and the quantity $\rho_0 \mathbf{k}$ enters the source of the tensorial continuity equation.

Considering in Equation (32) only one monomer, i.e., $\rho_0 = 1/V$, we get

$$\langle k_1^2 \rangle^0 = \frac{2k_B T}{3\epsilon l_0^2} \equiv \frac{2}{3} \frac{1}{l_0 \xi_p}, \quad (33)$$

where the superscript 0 stands for $k_B T/\epsilon \rightarrow 0$. One can verify that the same result as in Equation (33) is obtained directly by averaging the average square of the curvature in a given direction (Equation (31)) over all possible chain orientations, which corroborates the reasoning leading to Equation (32). In Equation (33) we have added the general connection between $\langle k_1^2 \rangle$ and the persistence length ξ_p of the chain [9, p. 399].

The above developments are approximate and rely on the assumption of small *collective* curvatures, which is correct for thermal fluctuations but cannot describe externally imposed arbitrary curvature conditions. In that case nonlinear effects become non-negligible and a more general theory would be needed.

C. Combined sources

Finally, we establish a model that describes both sources of the tensorial continuity constraint on a unified basis, with a single variable

$$\mathbf{h} = \mathbf{g} + \rho_0 l_0 \mathbf{k}, \quad (34)$$

analogous to what has been done in Ref. [3] for the chain ends and chain backfolds as the sources of the vectorial continuity constraint for the ‘‘recovered’’ polar order. This enables us to predict the strength G of the tensorial constraint, which is enforced simply by the unified source penalty potential in Equation (12) rather than by introducing additional system variables for the sources.

Following Equations (29) and (32), the total nonequilibrium free-energy density of the sources is

$$\Delta f(\mathbf{g}, \mathbf{k}) = \Delta f(\mathbf{g}) + \Delta f(\mathbf{k}) = \frac{1}{2} \left[\frac{3k_B T}{\rho_0^\pm} g^2 + \frac{3}{2} \frac{\epsilon l_0^2}{\rho_0} (\rho_0 k)^2 \right]. \quad (35)$$

Considering the combined source \mathbf{h} , its free-energy density is obtained by averaging Equation (35) over all possible realizations (Equation (34)) of \mathbf{h} ,

$$\Delta \bar{f}(\mathbf{h}) = -(1/V_1) d(\ln Z)/d\beta, \quad (36)$$

where $\beta = 1/(k_B T)$ and the partition function is given as

$$Z = \iint d^3 g d^3 k \mathcal{P}(\mathbf{g}) \mathcal{P}(\mathbf{k}) \delta(\mathbf{g} + \rho_0 l_0 \mathbf{k} - \mathbf{h}). \quad (37)$$

Here both $\mathcal{P}(\mathbf{g})$ and $\mathcal{P}(\mathbf{k})$ are thermal Boltzmann weights corresponding to energies $V_1\Delta f(\mathbf{g})$ and $V_1\Delta f(\mathbf{k})$, where V_1 is a coarse-graining volume that does not appear in the final result. To calculate the average in Equation (36), it is thus sufficient to calculate just the integral in Equation (37), which is carried out in spherical coordinates with $\mathbf{h} = h\hat{\mathbf{e}}_z$ and $\mathbf{g} \cdot \mathbf{h} = gh \cos \theta$. The result is

$$\Delta \bar{f}(h) = \frac{3k_B T}{2} \left(\frac{1}{V_1} + \frac{h^2}{\rho_0^\pm + 2k_B T \rho_0 / \epsilon} \right), \quad (38)$$

where the first, constant term $3k_B T / (2V_1)$ can be omitted — it arises due to the fact that the state $\mathbf{h} = 0$ can be realized by $\mathbf{g} = -\rho_0 l_0 \mathbf{k} \neq 0$, which costs energy (i.e., the ground state energy), while the second term is actually the free-energy density (Equation (35)) of the average source, in accord with the property of the Gaussian distribution $\overline{f(\bar{h})} = \overline{\Delta f(0)} + \Delta f(\bar{h})$.

Thus, the nonequilibrium free-energy density of the total effective source \mathbf{h} in arbitrary direction is $\Delta f(\mathbf{h}) = \frac{1}{2} G h^2$, where the result of the combined sources model for the coupling strength G that enters Equation (12) is

$$G = \frac{3k_B T}{\rho_0^\pm + 2k_B T \rho_0 / \epsilon}. \quad (39)$$

V. BEND OF MONOMER PAIRS

Here, we write down the general statistical result for the bending configuration of an independent monomer pair with bending energy of Equation (30).

In the stiff limit ($k_B T / \epsilon \ll 1$), the result in Equation (31) holds for the individual component of the curvature vector perpendicular to the monomers, and Equation (33) holds for the curvature in any direction in the case of isotropically averaged monomer orientation.

Conversely, in the ideally flexible limit ($k_B T / \epsilon \gg 1$) the chain undergoes a random walk. Putting $\mathbf{u}^i = \hat{\mathbf{e}}_z$ and $\mathbf{u}^{i+1} = \mathbf{u}^i + l_0 \mathbf{k}_0 = \hat{\mathbf{e}}_r$, we have

$$(l_0 k_0)^2 = 2(1 - \cos \theta) \quad (40)$$

and the solid angle average over all possible orientations of \mathbf{u}^{i+1} is $l_0^2 \overline{k_0^2} = 2$. Hence, in the isotropically averaged situation, the average square of the curvature in any direction is

$$\langle k_1^2 \rangle^\infty = \frac{1}{3} \overline{k_0^2} = \frac{2}{3} \frac{1}{l_0^2}, \quad (41)$$

where the superscript $^\infty$ stands for $k_B T / \epsilon \rightarrow \infty$.

For general flexibility, the partition function corresponding to the energy in Equation (30) is

$$Z = \int_{-1}^1 d(\cos \theta) e^{-\beta \Delta F(\theta)} = e^{-\beta \epsilon} \frac{2}{\beta \epsilon} \sinh \beta \epsilon, \quad (42)$$

where $\beta = 1 / (k_B T)$, and the average energy is

$$\langle \Delta F \rangle = -\frac{\partial}{\partial \beta} \ln Z = \frac{1}{\beta} - \epsilon (\coth \beta \epsilon - 1). \quad (43)$$

With that, using Equations (30) and (40) and furthermore taking into account the isotropy as done in Equation (41), the average square of the curvature in an arbitrary direction is $\langle k_1^2 \rangle = 2 / (3\epsilon l_0^2) \langle \Delta F \rangle$, such that

$$\frac{1}{\langle k_1^2 \rangle} = \frac{3}{2} l_0^2 \frac{\epsilon}{k_B T - \epsilon \left(\coth \frac{\epsilon}{k_B T} - 1 \right)}. \quad (44)$$

One can verify that the result in Equation (44) includes both the stiff chain limit (Equation (33)) and the flexible chain limit (Equation (41)).

Finally, the quantity $\langle k_1^2 \rangle$ can be determined from simulation data by measuring the average square of the curvature in an arbitrarily chosen direction. Figure S1 reveals a remarkable agreement between Equation (44) and $1 / \langle k_1^2 \rangle$ from the simulations. Thus, the exact statistical result for the isolated segment pair applies with great accuracy also to pairs surrounded by neighbouring chains of the simulated melt.

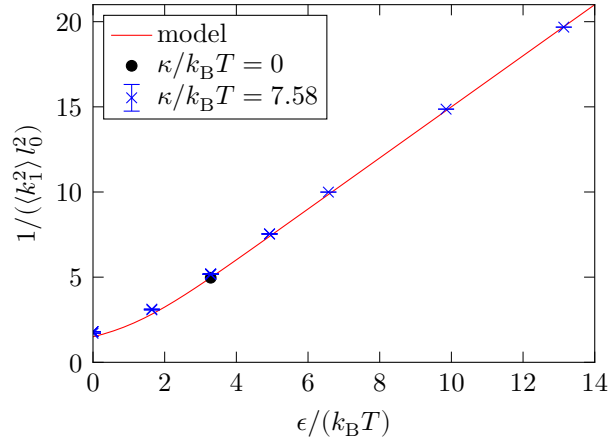


Figure S1. The values of $1/\langle k_1^2 \rangle$ from the simulations (points) for all studied chain lengths N_s , and plot (no fitting) of the model given by Equation (44). The extra circular point belongs to the simulation without the repulsive potential ($\kappa = 0$) and falls exactly onto the theoretical curve.

Moreover, the additional point in Figure S1 with the repulsive potential between all monomers switched off ($\kappa = 0$) indicates that the repulsion from other chains as well as the repulsion between the monomers forming the joint (correction to the bending rigidity ϵ) is small. Also small is apparently the influence of the continuity equation on the magnitude $|\delta \mathbf{k}|^2$ of its curvature source. Were this not the case, the large compressibility when $\kappa = 0$ would result in a significant change of $\langle k_1^2 \rangle$, as a result of the vanishing cost of density fluctuations that are coupled with fluctuations $\delta \mathbf{k}$ through the continuity constraint.

VI. INDUCED ORIENTATIONAL ORDER

The equilibrium coupling of the nematic order tensor to a given fixed density or concentration variation $\delta \rho(\mathbf{r})$ is obtained by minimizing the part of the free energy belonging to δQ_{ij} and the sources of the continuity constraint,

$$f' = \frac{1}{2}A(\delta Q_{ij})^2 + \frac{1}{2}L(\partial_k \delta Q_{ij})^2 + \frac{1}{2}G'[\rho \partial_j \delta Q_{ij} + (\delta Q_{ij} + \frac{1}{2}\delta_{ij})\partial_j \delta \rho]^2, \quad (45)$$

where $G' = G(\frac{2}{3}l_0)^2$, with the result

$$\frac{\delta f'}{\delta(\delta Q_{ij})} = 0 = A\delta Q_{ij} - L\partial_k^2 \delta Q_{ij} - G'\rho \partial_j [\rho \partial_k \delta Q_{ik} + (\delta Q_{ik} + \frac{1}{2}\delta_{ik})\partial_k \delta \rho], \quad (46)$$

$$p_k \frac{\partial f'}{\partial(\partial_k \delta Q_{ij})} \Big|_{\partial} = 0 = L\partial_k \delta Q_{ij} \Big|_{\partial} p_k + G'\rho [\rho \partial_k \delta Q_{ik} + (\delta Q_{ik} + \frac{1}{2}\delta_{ik})\partial_k \delta \rho] \Big|_{\partial} p_j, \quad (47)$$

where, in case relevant, Equation (47) holds at the bounding surface with the normal \mathbf{p} . For the reason of generality, the non-linearized continuity constraint has been considered in Equation (45).

We have already seen via the Fourier space that a density (acoustic) plane wave $\delta \tilde{\rho}(\mathbf{r}, t) = \delta \rho(\mathbf{r}, t)/\rho_0$ with wave vector $\mathbf{q} = q\hat{\mathbf{e}}_z$ couples only to the component δQ_{zz} . Taking $\nabla = \hat{\mathbf{e}}_z \partial_z$ in Equation (46) and linearizing it, we get

$$\delta Q_{zz}(\mathbf{r}, t) = -\frac{1}{2} \frac{\tilde{G}q^2}{A + (L + \tilde{G})q^2} \delta \tilde{\rho}(\mathbf{r}, t). \quad (48)$$

In polymer solutions, $\delta \tilde{\rho}$ represents concentration variations rather than variations of the density. In the one-dimensional case where the externally imposed concentration gradient is along z , Equation (46) leads to

$$(L + G'\rho^2)\partial_z^2 \delta Q_{zz} + 2G'\rho(\partial_z \delta \rho)\partial_z \delta Q_{zz} + G'(\delta Q_{zz} + \frac{1}{2})\rho \partial_z^2 \delta \rho - A\delta Q_{zz} = 0. \quad (49)$$

If the relevant range is $-d/2 < z < d/2$ and we for simplicity assume that $|\partial_z \delta \rho| d / \rho \ll 1$, the homogeneous solution of Equation (49), i.e., the solution for constant $\partial_z \delta \rho$, is of the simple form $\delta Q_{zz}(z) = C_1 e^{\lambda_1 z} + C_2 e^{\lambda_2 z}$, with real

$$\lambda_{1,2} = \frac{-G' \rho \partial_z \delta \rho \pm \sqrt{(G' \rho \partial_z \delta \rho)^2 + A(L + G' \rho^2)}}{L + G' \rho^2}. \quad (50)$$

The relevant regime is that of weak density–nematic coupling and small concentration gradient, such that $(G' \rho \partial_z \delta \rho)^2 \ll A(L + G' \rho^2)$ holds and $\lambda_{1,2} \rightarrow \pm \sqrt{A/L} = \pm \xi^{-1}$. Note that this limit is equivalent to linearizing Equations (46) and (47) with respect to δQ_{ij} and $\delta \rho$. Hence, in a good approximation the solution is further simplified, and with the choice $\delta Q_{zz}(z=0) = 0$ becomes

$$\delta Q_{zz}(z) \approx C_1 \sinh \lambda_1 z. \quad (51)$$

The boundary condition at $z = d/2$ (or, equivalently, $z = -d/2$) follows from linearized Equation (47),

$$\partial_z \delta Q_{zz}(d/2) = -\frac{1}{4} \frac{G' \rho \partial_z \delta \rho}{L + G' \rho^2}, \quad (52)$$

so that finally we have

$$\delta Q_{zz}(z) \approx -\frac{G' \rho \partial_z \delta \rho}{4 \lambda_1 (L + G' \rho^2)} \frac{\sinh \lambda_1 z}{\cosh(\lambda_1 d/2)}. \quad (53)$$

That is, as a response to a constant concentration gradient, δQ_{zz} is modulated in the boundary layers with characteristic thickness of the nematic correlation length ξ .

When the concentration gradient is not constant, $\partial_z^2 \delta \rho$ presents an inhomogeneity in Equation (49). If $\partial_z \delta \rho(z)$ is a slowly varying function (on the scale of ξ), we get from Equation (49) in the limit $\delta Q_{zz} \rightarrow 0$

$$\partial_z^2 Q_{zz} \approx -\frac{1}{2} \frac{G' \rho}{L + G' \rho^2} \partial_z^2 \delta \rho, \quad (54)$$

which thus represents the drive of the induced nematic ordering.

If the polymer concentration is spherically symmetric, one expects a uniaxial ordering of the chains in the radial direction and can write, without loss of generality, in spherical coordinates (r, θ, ϕ)

$$\mathbf{Q}(\mathbf{r}) = Q_{rr}(r) [\hat{\mathbf{e}}_r \otimes \hat{\mathbf{e}}_r - \frac{1}{2} (\hat{\mathbf{e}}_\theta \otimes \hat{\mathbf{e}}_\theta + \hat{\mathbf{e}}_\phi \otimes \hat{\mathbf{e}}_\phi)] \equiv Q_{rr}(r) \mathbb{T}(\mathbf{r}). \quad (55)$$

With $\nabla = \hat{\mathbf{e}}_r \frac{\partial}{\partial r} + \hat{\mathbf{e}}_\theta \frac{\partial}{r \partial \theta} + \hat{\mathbf{e}}_\phi \frac{\partial}{r \sin \theta \partial \phi}$, the nonzero derivatives of the spherical base vectors and some algebra we find the auxiliary expressions

$$\nabla \cdot \mathbf{Q} = \left(\partial_r Q_{rr} + \frac{3}{r} Q_{rr} \right) \hat{\mathbf{e}}_r, \quad (56)$$

$$\nabla^2 \mathbf{Q} = \frac{1}{r^2} \frac{\partial}{\partial r} \left(r^2 \frac{\partial Q_{rr}}{\partial r} \right) \mathbb{T} - \frac{6}{r^2} Q_{rr} \mathbb{T}. \quad (57)$$

It is sufficient to take only the $\hat{\mathbf{e}}_r$ -part of the gradient (denoted ∂_j) in Equation (46),

$$G' \rho \partial_r \left(\rho \partial_r Q_{rr} + \frac{3}{r} \rho Q_{rr} + (Q_{rr} + \frac{1}{2}) \partial_r \rho \right) \hat{\mathbf{e}}_r \otimes \hat{\mathbf{e}}_r - A Q_{rr} \mathbb{T} + \frac{1}{r^2} L [\partial_r (r^2 \partial_r Q_{rr}) - 6 Q_{rr}] \mathbb{T} = 0, \quad (58)$$

and consider the component along $\hat{\mathbf{e}}_r \otimes \hat{\mathbf{e}}_r$, which one gets simply by dropping all tensors in Equation (58), since $\hat{\mathbf{e}}_r \cdot \mathbb{T} \cdot \hat{\mathbf{e}}_r = 1$.

If the polymer concentration is of the specific form given by $\rho(r) = \rho_0 - \Phi / (4\pi D r)$, we have $\partial_r^2 \rho = -2\Phi / (4\pi D r^3)$. Using the same approximations as for Equation (54), which are $\rho \approx \rho_0$, $\{(G' \rho_0 \partial_r \rho)^2, (G' \rho_0^2 / r)^2\} \ll A(L + G' \rho^2)$ and $Q_{rr} \equiv \delta Q_{rr} \rightarrow 0$, from Equation (58) we finally get

$$(L + G' \rho_0^2) \partial_r^2 \delta Q_{rr} + \frac{2L + 3G' \rho_0^2}{r} \partial_r \delta Q_{rr} - \frac{6L}{r^2} \delta Q_{rr} = G' \rho_0 \frac{\Phi}{4\pi D r^3}. \quad (59)$$

Using a power-law ansatz, the solution is

$$\delta Q_{rr}(r) \approx -\frac{G' \rho_0}{6L + G' \rho_0^2} \frac{\Phi}{4\pi D r}. \quad (60)$$

-
- [1] D. Svenšek, G. M. Grason, R. Podgornik, *Phys. Rev. E* **2013**, *88*, 052603.
 - [2] P. Gemünden, K. C. Daoulas, *Soft Matter* **2015**, *11*, 532–544.
 - [3] A. Popadić, D. Svenšek, R. Podgornik, K. C. Daoulas, M. Praprotnik, *Soft Matter* **2018**, *14*, 5898–5905.
 - [4] K. C. Daoulas, V. Rühle, K. Kremer, *J. Phys. Condens. Matter* **2012**, *24*, 284121.
 - [5] C. Greco, Y. Jiang, J. Z. Y. Chen, K. Kremer, K. C. Daoulas, *J. Chem. Phys.* **2016**, *145*, 184901.
 - [6] D. Frenkel, B. Smit, *Understanding Molecular Simulation: From Algorithms to Applications*, Academic Press, San Diego, 2nd ed., **2001**.
 - [7] M. Tuckerman, *Statistical Mechanics: Theory and Molecular Simulation*, Oxford University Press, Oxford, **2010**.
 - [8] M. P. Allen, D. J. Tildesley, *Computer Simulation of Liquids*, Clarendon Press, Oxford, **1990**.
 - [9] L. D. Landau, E. M. Lifshitz, *Statistical Physics, Vol. 5*, Butterworth-Heinemann, Oxford, 3rd ed., **1980**.